Geophysical Journal International

Geophys. J. Int. (2020) **220,** 1275–1283
Advance Access publication 2019 November 05
GJI Geodynamics and tectonics

doi: 10.1093/gji/ggz502

Variations in mantle lithosphere buoyancy reveal seismogenic behaviour in the Sunda–Andaman subduction zone

Wen-Bin Doo [1], Chung-Liang Lo,[1] Hao Kuo-Chen [2], Yin-Sheng Huang,[1] Wen-Nan Wu,[3] Shu-Kun Hsu[1,2] and Hsueh-Fen Wang[1]

[1] *Center for Environmental Studies, National Central University, Taoyuan City, 32001, Taiwan. E-mail: wenbindoo@gmail.com*
[2] *Department of Earth Sciences, National Central University, Taoyuan City, 32001, Taiwan*
[3] *College of Oceanography, Hohai University, Nanjing City, 210098, China*

Accepted 2019 November 1. Received 2019 October 24; in original form 2019 May 9

SUMMARY

The distribution of historic earthquakes in the Sumatra subduction zone reveals, in the forearc region, the intense seismic activity and frequent occurrences of $M_w > 8$ earthquakes throughout the whole area. In contrast, the neighbouring region has less dense seismicity and no large earthquake greater than M_w8 has been observed in the Java subduction zone. Such different seismic behaviours may be due to distinct degrees of the stress accumulation and release. In this study, the strength of plate coupling inferred from mantle lithosphere buoyancy (H_m) estimation is used to explain the seismogenic behaviour in the Sunda–Andaman subduction zone. Strong and weak plate coupling status are obtained in the Sumatra and Java subduction zones, respectively. These results can explain the significant differences in seismogenic behaviours in the Sunda–Andaman subduction zone. In assessing the global implications of this finding, we observe that uplifted serpentinized forearc mantle peridotite is the critical phenomenon in weak plate coupling cases and leads to a limit on the width of the coupling zone. Strong plate coupling can cause a relatively low gravity anomaly as well as a negative trench-parallel gravity anomaly (TPGA) in the forearc regions and correlates well with the occurrence of large earthquakes, whereas weak plate coupling can cause a positive TPGA and constrain the potential occurrence of large earthquakes.

Key words: Gravity anomalies and Earth structure; Earthquake source observations; Dynamics: gravity and tectonics; Dynamics: seismotectonics; Subduction zone processes.

1 INTRODUCTION

Subduction zones are plate tectonic boundaries. They accumulate stress as one plate moves over another and then catastrophically release this stress in one or more earthquakes along what is commonly referred to as the seismogenic zone. Approximately 90 per cent of the world's earthquakes and almost all large magnitude (M_w8 or greater) events occur along subduction zones. These events are major threats to human societies and economies. Their occurrence, therefore, motivates efforts to identify the subduction zones that may generate catastrophic events. In general, the recurrence intervals of large earthquakes may range from several hundred years (Japan Trench; Satake 2015) to over 400 yr (Sumatra; Ando *et al*. 2009). Seismicity catalogues alone may not adequately indicate the recurrence intervals of large earthquakes. The seismogenic characteristics of subduction zones need to be further investigated. However, the seismogenic behaviour of many subduction zones remains poorly understood due to the limited spatial coverage of seismic networks and geodetic data. Approaches for acquiring additional observations and conducting theoretical studies (independent methods from seismicity) are worthwhile because they may provide new constraints for evaluating the seismic potential in subduction zones. Previous studies have proposed that along-trench variations in some parameters, such as the convergence rate, age of the oceanic plate (Ruff & Kanamori 1980; Kanamori 1986) and backarc spreading (Uyeda & Kanamori 1979), may influence seismogenic behaviour. However, Ando *et al*. (2009) have suggested that the correlation between these processes and the generation of large subduction zone earthquakes is weak. Recently, many other parameters (and/or methods) have been reported to discuss the seismogenic behaviour in subduction zones, such as trench-parallel gravity anomalies (TPGA; Song & Simons 2003; Wells *et al*. 2003; Hsu *et al*. 2012), trench sediment thickness (Ruff 1989; Scholl *et al*. 2011, 2015; Heuret *et al*. 2012; Seno 2017; Brizzi *et al*. 2018), mechanical and material properties of subducted sediments (Hyndman *et al*. 1997; Peacock & Hyndmn 1999) and plate coupling (deduced from GPS data; Simoes *et al*. 2004; Chlieh *et al*. 2008; Konca *et al*. 2008; Tadokoro *et al*. 2018). Understanding

these variations may help to evaluate seismic hazards in subduction zones.

The occurrence of subduction zone earthquakes is controlled by the state of stress on the interface between the subducting and overriding plates (Nishikawa & Ide 2014). Intuitively, stress is more easily accumulated, and greater amounts of seismic energy can be released to produce earthquakes where the subducting and overriding plates are strongly coupled (or locked) in a subduction zone. However, the direct measurement of the stress state on a plate interface is difficult. The strength of plate coupling describes the interaction between an overriding plate and the associated subducting plate and can be evaluated by determining the buoyancy of the mantle lithosphere ($H_{m;}$ Gvirtzman & Nur 1999a). The method of determining H_m has been applied to several subduction zones (Gvirtzman & Nur 1999a,b, 2001; Hsu 2001; Lo *et al*. 2017; Doo *et al*. 2018). In the Sunda–Andaman subduction zone, the seismicity distributions show significant spatial variations; the potential of great destructive earthquakes is larger for Sumatra than Java (Fig. 1). In this study, we calculated H_m for four density profiles (across the Sumatra and Java subduction zones) to enable the discussion of the relationship between the strength of plate coupling and the occurrence of large earthquakes in the Sunda–Andaman subduction zone.

2 SEISMIC CHARACTERISTICS IN THE SUNDA–ANDAMAN SUBDUCTION ZONE

The Sunda–Andaman subduction zone, where the Indo-Australian plate subducts beneath the Eurasian plate, is a seismically region. The rate of plate convergence decreases westwards from 80 mm yr^{-1} off Java to 55 mm yr^{-1} off the coast of northern Sumatra (DeMets *et al*. 1994). The convergence direction is nearly orthogonal along the Java trench and becomes oblique in the Andaman–Sumatra section. In addition, the age of the subducting oceanic crust varies from 40–60 Ma off Sumatra to 70–120 Ma off Java (Müller *et al*. 2008). The spatial distribution of earthquakes recorded by the global centroid moment tensor (GCMT) catalogue (Dziewonski *et al*. 1981) as having occurred in the Sunda–Andaman subduction zone between 1976 January 1 and 2015 April 30 suggests that the seismic potential for a large earthquake to occur off Sumatra is much larger than that for Java (Fig. 1). Three large earthquakes ($M_w > 8$) and a number of M_w7 events have occurred in the Sumatra subduction zone in the last decade. The most destructive of these earthquakes, the 2004 December 26 M_w9.3 event, occurred in the northern Sumatra subduction zone and caused a deadly tsunami. South of the 2004 event, the 2005 March 28 M_w8.7 earthquake (Konca *et al*. 2008) ruptured the same region as the 1861 event ($M \sim 8.5$; Newcomb & McCann 1987; Natawidjaja *et al*. 2004). Moreover, two large historical earthquakes occurred around the Mentawai Islands (pink triangle shown in Fig. 1) and caused destructive tsunamis in 1797 ($M_w \sim 8.8$) and 1833 ($M_w \sim 9.0$) (Newcomb & McCann 1987; Natawidjaja *et al*. 2006). In contrast to the relatively high frequency occurrence of large earthquakes along the Sumatra segment, in the adjacent area shown in Fig. 1, only two $M_w > 7$ events have occurred in the Java subduction zone, and no $M_w > 7$ event has been observed in the forearc area. In addition, the M_w7.8 earthquake in 1994 was related to a subducting seamount (Abercrombie *et al*. 2001). Unlike Sumatra, the Java subduction zone is suggested to have low seismic potential (Newcomb & McCann 1987). Based on the observed seismic behaviour in the Sumatra and Java subduction zones, we expect that the processes by which seismic stress accumulates and is released and the subsurface structural characteristics may differ between these two subduction zones. Understanding the local differences between these zones may produce insight that could be applied to other subduction zones.

Grevemeyer & Tiwari (2006) performed forward gravity modelling along four profiles (P1–P4) perpendicular to the strike of the trench (Fig. 1). The geometry of each profile was initially constrained by seismic refraction and earthquake data. Seismic refraction data constrain the shallow depth (∼15 km) and earthquake data constrain greater depth of the subducting plate. Both incoming oceanic crust and subducting oceanic crust are kept constant at ∼7 km thickness. Four density profiles were modified to fit the observed gravity anomalies; then, obtained the final density models (Fig. 2). As shown in Fig. 2, the main subsurface structural difference between Sumatra and Java is the shallow mantle wedge. According to these four density profiles, we can estimate mantle lithosphere buoyancy across the Sumatra and Java subduction zones.

3 BUOYANCY OF MANTLE LITHOSPHERE (H_m)

In this study, we evaluate the strength of plate coupling inferred from the estimation of H_m (Gvirtzman & Nur 1999a). Here, we provide a brief introduction to this method. For additional details on this method, readers can refer to the literature (Gvirtzman & Nur 1999a,b, 2001). Under the condition of isostatic equilibrium, the mean elevation of a region can be determined as follows:

$$\varepsilon = \mathrm{a}(H_c + H_m - H_0)$$
$$\mathrm{a} = 1 \text{ for } \varepsilon \geq 0$$
$$\mathrm{a} = \frac{\rho_\alpha}{\rho_\alpha - \rho_w} \text{ for } \varepsilon < 0 \quad (1)$$

where ε is the surface elevation; ρ_α and ρ_w are the densities of the asthenosphere and sea water, respectively; H_c and H_m are the buoyancy of the crust and the mantle lithosphere, respectively; and $H_0 \approx 2.4$ km is a reference constant for the buoyant height of sea level at a mid-ocean ridge associated with the densities in eq. (1); all above refer to the free asthenosphere surface (Lachenbruch & Morgan 1990):

$$H_c = \frac{1}{\rho_\alpha}(\rho_\alpha - \rho_c)L_c \quad (2)$$

$$H_m = \frac{1}{\rho_\alpha}(\rho_\alpha - \rho_m)L_m, \quad (3)$$

where ρ_c and ρ_m are the densities and L_c and L_m are the thicknesses of the crust and mantle lithosphere, respectively. If we assume that the region is in isostatic equilibrium, then the surface elevation is contributed from the buoyancy of the crust (H_c) and the mantle lithosphere (H_m). H_c can be estimated according to the density model and crustal geometry; then, the changes in surface elevation are associated with the value of H_m (eq. 1). However, in subduction zones, the topography is lowered by the drag of the descending slab (coupled) or uplifted by overriding plate rebounding due to the overriding plate is detached from the subducted plate (decoupled). The residual topography (observed topography minus H_c), therefore, reflects the contribution from the buoyancy of mantle lithosphere and the forces that are pulled down by descending slabs or uplifted by the ascending asthenospheric materials. In other words, near a convergent plate boundary, the change of the residual topography depends on the status of plate coupling and is revealed by variation in H_m (Gvirtzman & Nur 1999a).

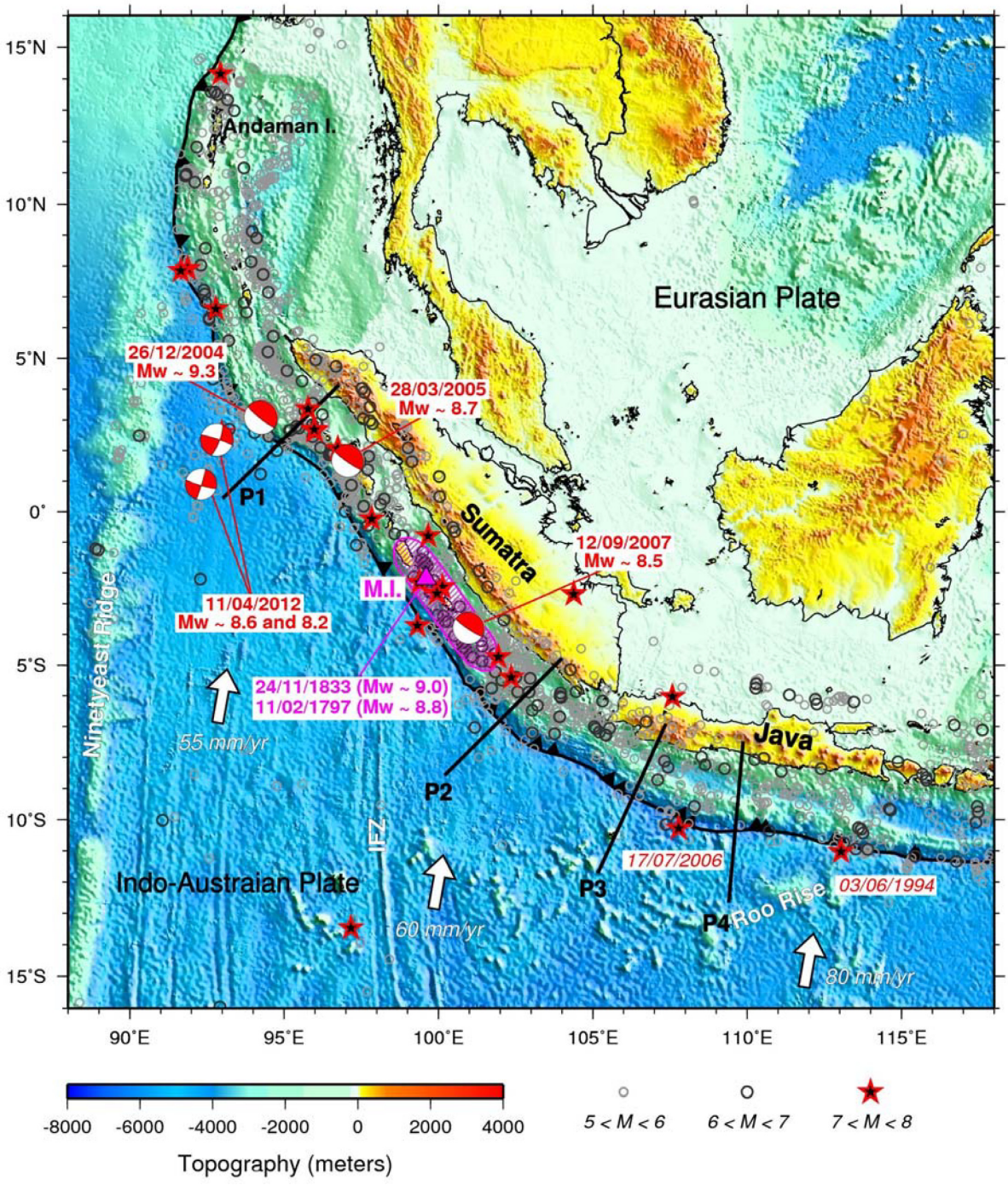

Figure 1. Seismicity distribution map of the Sunda–Andaman subduction zone. Earthquake data were obtained from the Global CMT project (1976 to April 2015) data catalogue ($M_w > 5$). The thick white arrows indicate the relative motion between the Indo-Australian and Eurasian plates (DeMets *et al*. 1994). The pink triangle indicates the possible location of two past large earthquakes (1797 and 1833) and the pink area indicates the associated rupture area. P1–P4 (thick black lines) represent the profiles that we used to estimate the buoyancy of mantle lithosphere (H_m) in this study. IFZ: Investigator Fracture Zone; M.I.: Mentawai Islands.

4 STRENGTH OF PLATE COUPLING IN THE SUMATRA AND JAVA SUBDUCTION ZONES

Gvirtzman & Nur (1999a) showed that where an overriding plate is detached from the associated subducting plate, the H_m curve across the subduction zone displays a sharp variation (Calabria case in Fig. 3), which indicates weak plate coupling. In contrast, small variations in the H_m curve across a subduction zone indicate that a large portion of the overriding plate is coupled to the slab (strong plate coupling), as in the Andes subduction zone (Fig. 3). In addition, the H_m curves across the Bonin and Kurile arcs represent examples of intermediate coupling. Whereas the amplitude of the H_m variations there are as large as in Calabria, but, their wavelength is twice as long. In this study, our results show that the variations

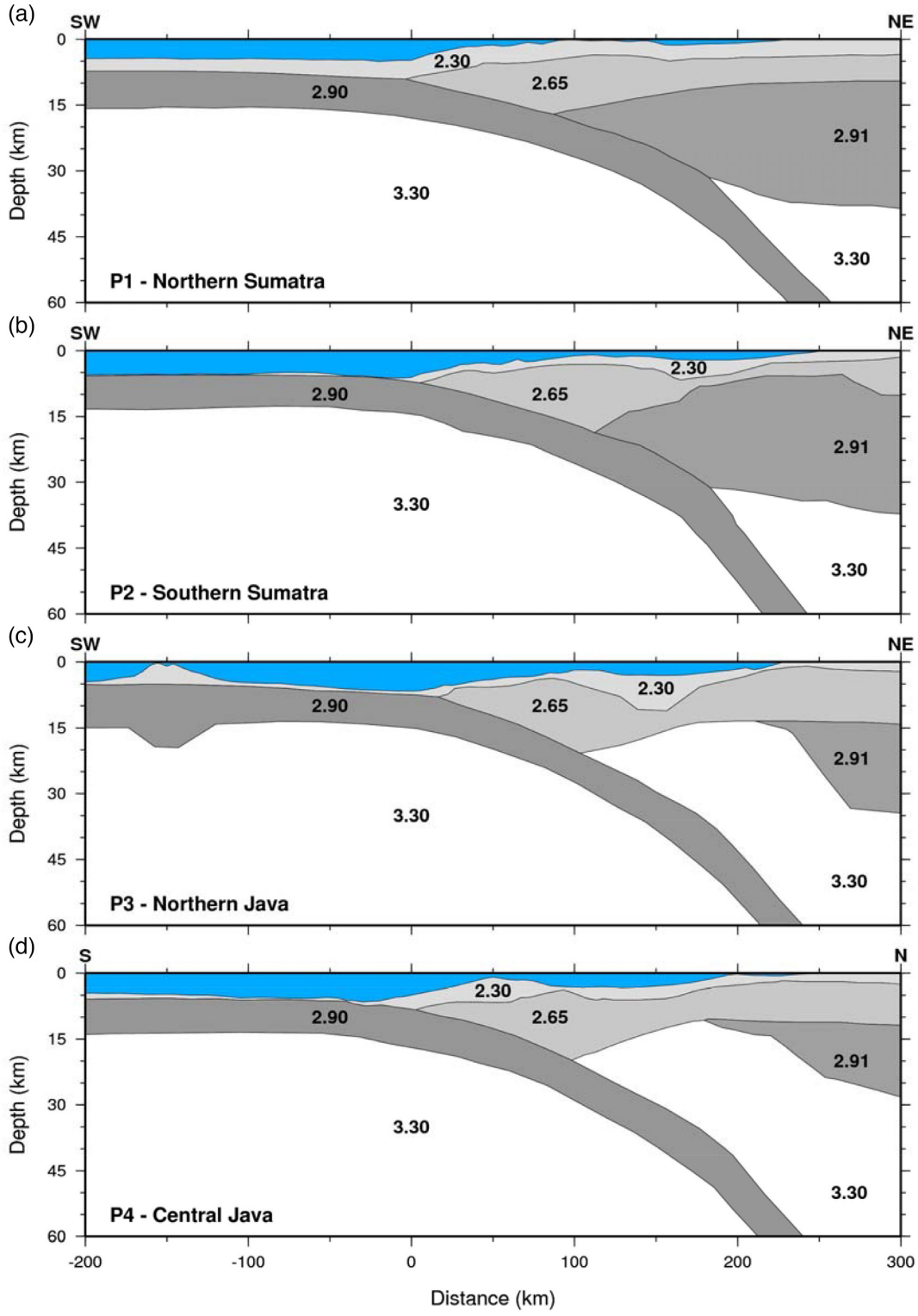

Figure 2. Density model of four profiles (P1–P4) across the Sumatra and Java subduction zones [modified from Grevemeyer & Tiwari (2006)].

in the H_m curve across the northern part of the Sumatra subduction zone (profile P1) are similar to those seen in the Andes subduction zone. The variations in the H_m curve across the southern part of the Sumatra subduction zone (profile P2) are not as small as those in the Andes subduction zone; however, they are much smaller than those observed in subduction zones that feature de-coupling (blue dashed line in Fig. 3). In other words, the overriding plate is still firmly coupled with the slab along the Sumatra subduction zone. In contrast, the variations in the H_m curve across the northwestern and central portions of the Java trench are large (profiles P3 and P4), exceeding the normal range associated with coupled plates, and similar to those seen in the Calabria subduction zone, implying that the plate

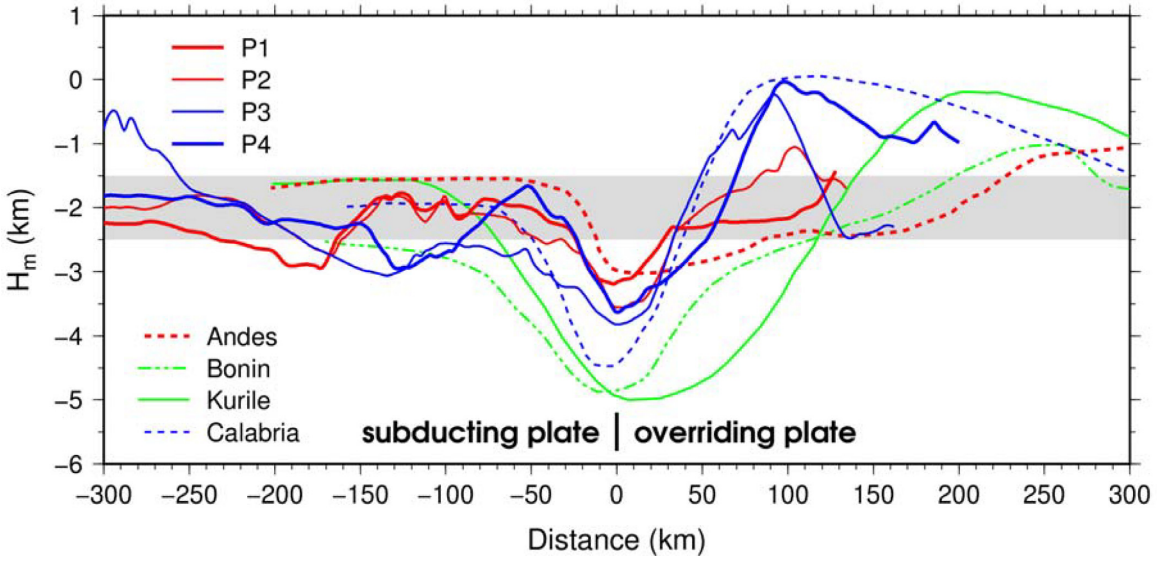

Figure 3. Map showing curves of H_m. The curves corresponding to P1–P4 represent the results of estimating H_m in this study. The curves corresponding to the Andes, Calabria, Izu-Bonin and Kurile are modified from Gvirtzman & Nur (1999a). The Andes represents a case of strong plate coupling. Calabria represents a case featuring weak plate coupling. Izu-Bonin and Kurile display intermediate anomalies. The grey band zone (2.0 ± 0.5) indicates the variations in H_m along the North America passive margin, which represents the normal contribution of the mantle lithosphere to the Earth's topography.

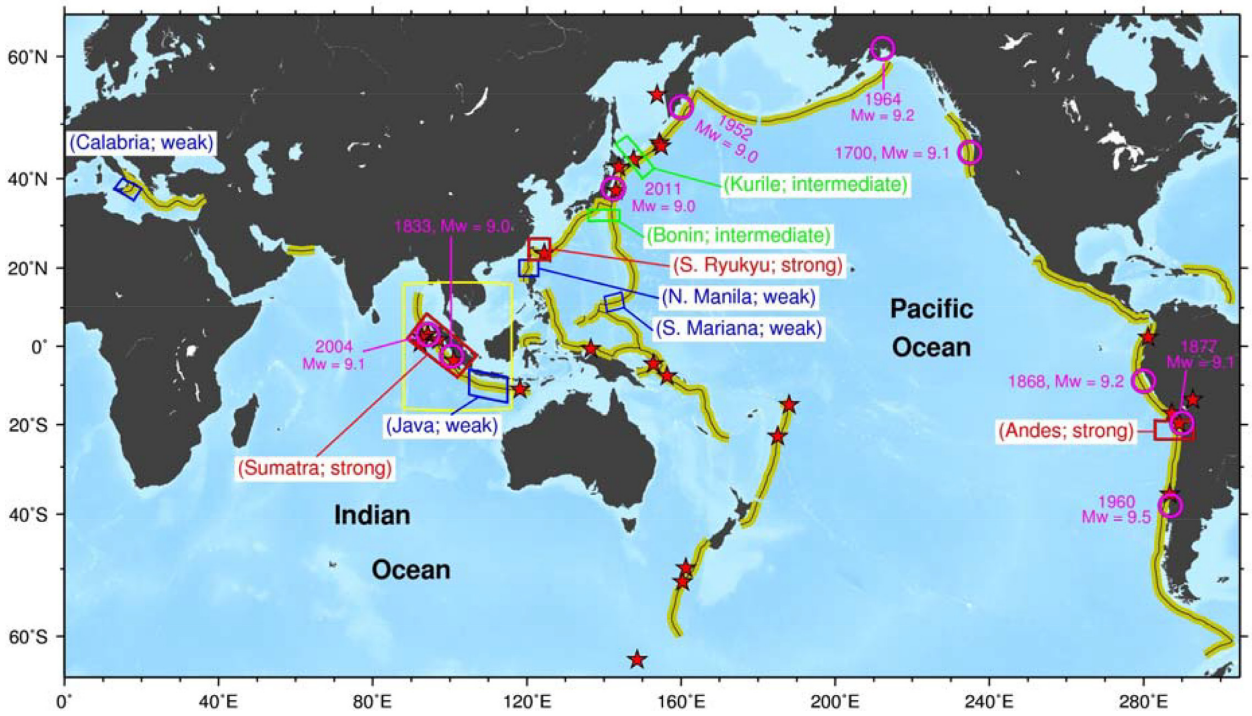

Figure 4. Map showing the locations of major subduction zones. The earthquake data, which show events with magnitudes larger than 8.0, were obtained from the GCMT project (1976 to April 2015) data catalogue. The pink circles indicate M_w9.0 or larger earthquakes that occurred between 1700 and 2017. The thick brown lines indicate the locations of subduction zones. The red, green and blue frames indicate the areas for which the strength of plate coupling is already known (Gvirtzman & Nur 1999a; Lo *et al*. 2017; Doo *et al*. 2018; this study).

coupling is weak there. These results could imply that the stresses accumulating and releasing in Sumatra are larger than those in Java. Several previous studies (Simoes *et al*. 2004; Chlieh *et al*. 2008; Konca *et al*. 2008) suggested that overriding and subducting plates are locked (or coupled) in the Sumatra subduction zone according to Global Positioning System (GPS) measurements. In contrast to the Sumatra trench, the seismicity along the Java trench is dominated by normal faulting earthquakes in the subducting plate Abercrombie *et al*. (2001) thus suggested that the two plates are poorly coupled. In addition, Grevemeyer & Tiwari (2006) suggested that the width of the coupling zone is larger in Sumatra than that in Java. We thus propose that the differences in seismogenic behaviour in the

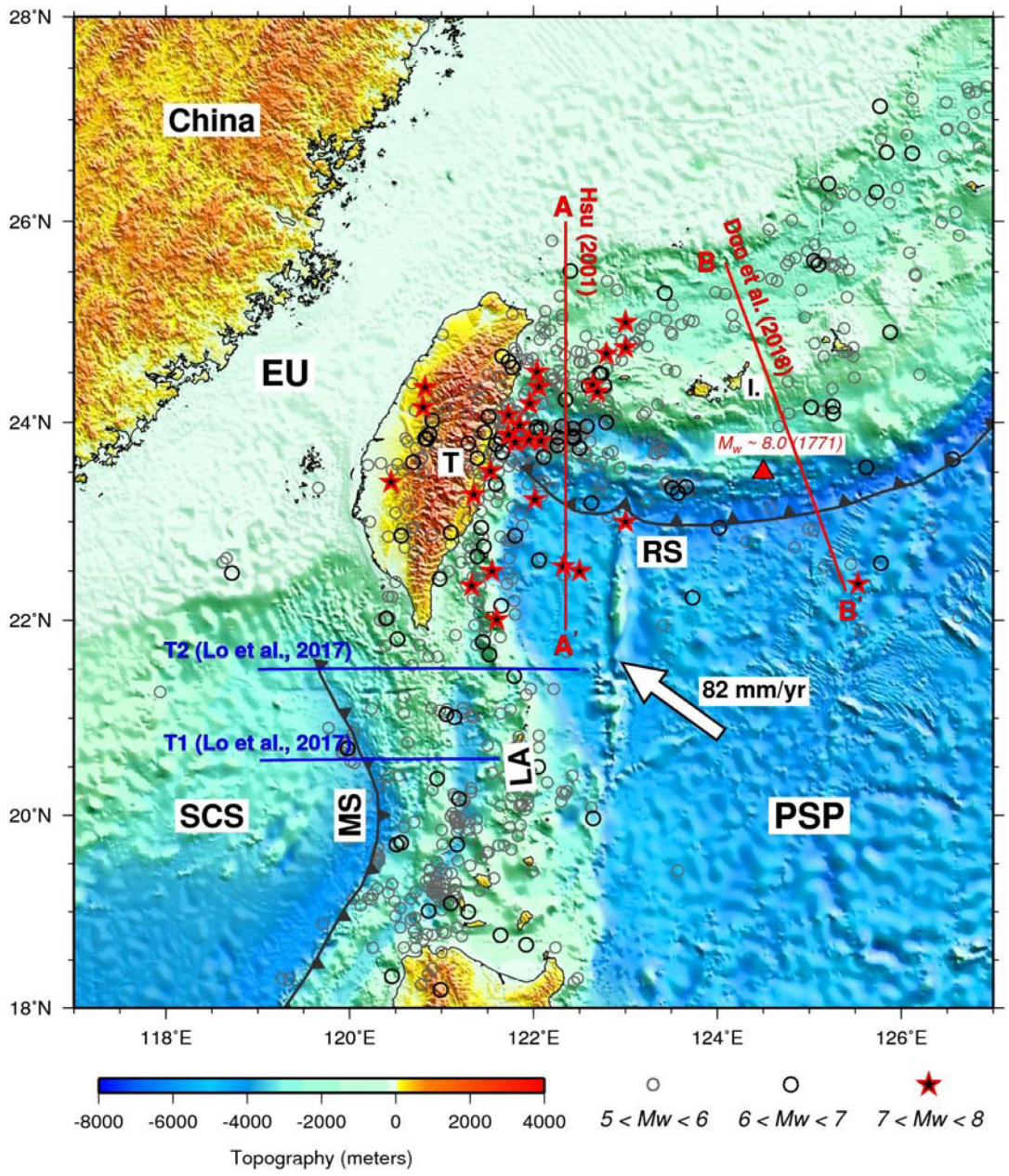

Figure 5. Map showing the distribution of seismic events near Taiwan area. The earthquake data were drawn from Global CMT and Theunissen *et al*. (2010). The red triangle indicates the possible location of the 1771 Yaeyama Japan earthquake (Nakamura 2009). The thick white arrows indicate the relative motion between the Philippine Sea and Eurasian plates. The H_m results indicate relatively strong and weak plate coupling status in the southern Ryukyu (profiles AA′ and BB′) and the northern Manila (profiles T1 and T2) subduction zones, respectively (Hsu 2001; Lo *et al*. 2017; Doo *et al*. 2018). EU: Eurasian plate; LA: Luzon Arc; MS: Manila subduction zone; PSP: Philippine Sea plate; RS: Ryukyu subduction zone; SCS: South China Sea.

Sunda–Andaman subduction zone can be explained by variations in the strength of plate coupling, as revealed by mantle lithosphere buoyancy.

5 DISCUSSION

By summarizing all of the published and new H_m results, in terms of the strength of plate coupling and the spatial distribution of large earthquakes in subduction zones, we find that areas with strong plate coupling are highly correlated with the occurrence of large earthquakes, whereas areas that display weak plate coupling are relatively aseismic (Fig. 4). Determining mantle lithosphere buoyancy could be a useful method of assessing large earthquake potential in subduction zones. However, 2-D profiles just reveal the local plate coupling strength and could not fully represent plate coupling status for the whole subduction zone, that is, it only indicates the condition in that segment of the subduction zone. The variations of the subsurface structural geometries along the subduction zone could be one of the major factors to influence H_m. In this section, we compare the subsurface structural characteristics of these two typical cases (strong and weak) and further discuss their implications.

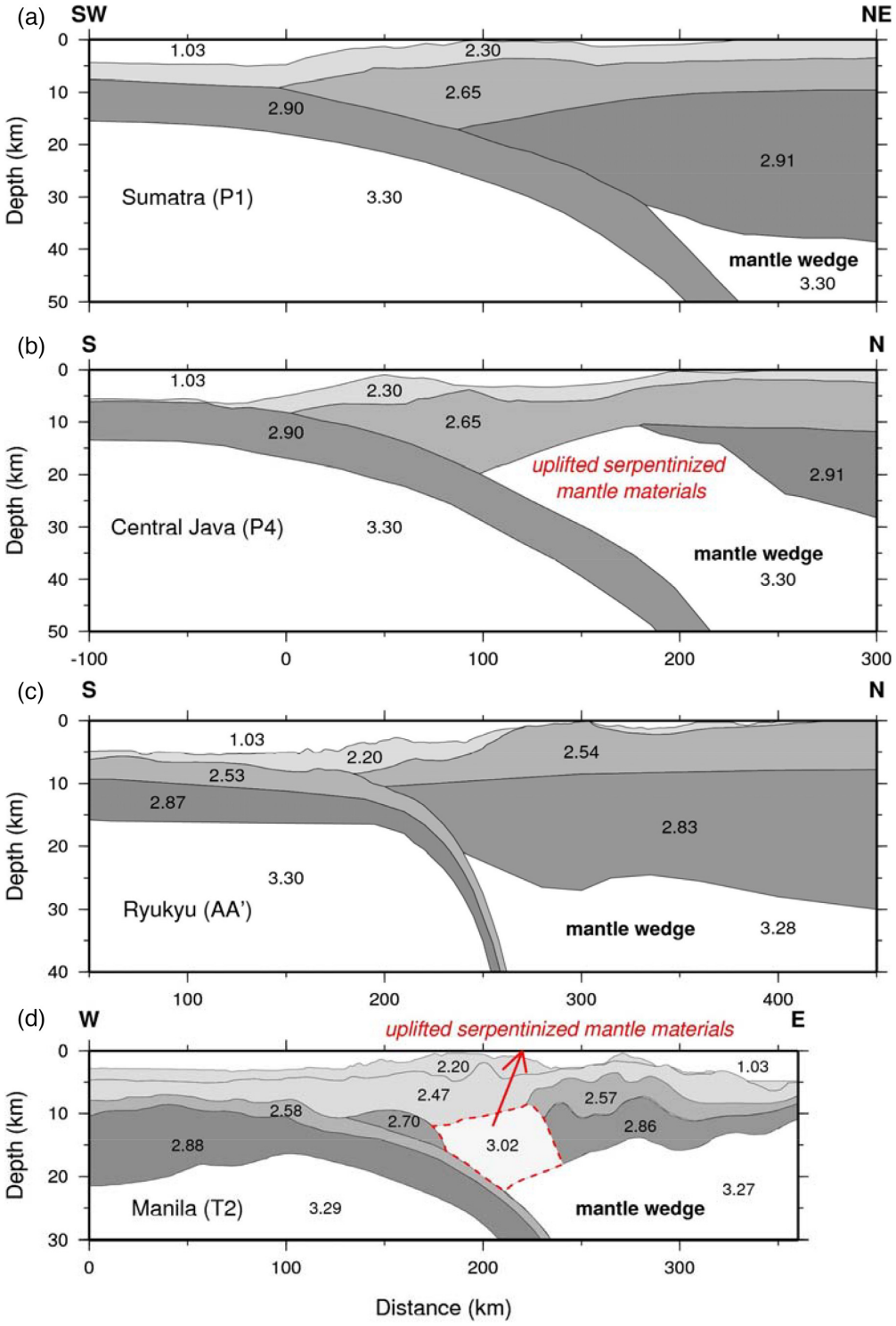

Figure 6. Map shows the structural geometries of the profiles. (a) Density structure of profile P1 [identified from Grevemeyer & Tiwari (2006)]. (b) Density structure of profile P4 [identified from Grevemeyer & Tiwari (2006)]. (c) Density structure of profile AA′ [identified from Hsu (2001)]. (d) Density structure of profile T2 [identified from Doo *et al*. (2015)]. Location of profiles P1 and P4 are shown in Fig. 1. Location of profiles AA′ and T2 are shown in Fig. 5. The numbers indicate the density of each block.

5.1 Weak plate coupling and uplifted serpentinized mantle

Subduction zones generate almost earthquakes above magnitude 8.0; however, rupture characteristics are highly individual and linked to margin specific geometric conditions (Koop 2013). Understanding subsurface structural characteristics can help us to assess the seismic potential in subduction zones. Previous studies (Hsu 2001; Lo *et al*. 2017; Doo *et al*. 2018) have determined mantle lithosphere buoyancy in the southern Ryukyu and northern Manila subduction zones, where the seismicity distributions show significant spatial variations (Fig. 5). They proposed strong and weak plate

coupling status in the southern Ryukyu and northern Manila subduction zones, respectively. In addition, their results provide constraints on the geometry of the crust in these two subduction zones and offer an opportunity to identify the difference between them. The structural evidence shown in Fig. 6 clearly indicates that the main subsurface structural difference between cases displaying strong (Figs 6a and c) and weak (Figs 6b and d) plate coupling is the uplift of a mantle wedge into the plate contact zone. In terms of the mechanism of serpentinization in a forearc mantle wedge, this phenomenon is both expected and observed in subduction zones (Zhao 2001; Bostock *et al*. 2002; Brocher *et al*. 2003; Hyndman & Peacock 2003; Pilchin 2005; Doo *et al*. 2015). The serpentinization of mantle rocks can reduce their seismic velocity and density (Bostock *et al*. 2002; Hyndman & Peacock 2003). Low-velocity and low-density anomalies are often interpreted as associated with the degree of serpentinization of the forearc mantle (Zhao *et al*. 2001; Bostock *et al*. 2002; Hyndman & Peacock 2003). Here, we find that the position of the serpentinized mantle materials plays an important role. In weak plate coupling cases, the overriding plate is detached from the subducted plate (Gvirtzman & Nur 1999a) and then creates space; this process facilitates the automatic uplift of serpentinized mantle materials into the plate contact zone due to its positive buoyancy (Doo *et al*. 2015). The presence of uplifted serpentinized mantle materials would limit the widths of the coupling zone and may therefore limit the sizes of rupture zones and the magnitudes of earthquakes. This observation may explain why areas with weak plate coupling have generally lower potential of large earthquake occurrence (as shown in Fig. 4). In addition, we would like to emphasize that weak plate coupling may be the critical factor in this process. This phenomenon (which we note in the Java and northern Manila subduction zones) is similar to the Calabria case of Gvirtzman & Nur (1999a), where weak plate coupling is present.

5.2 Relationships between plate coupling, trench-parallel gravity anomalies and large earthquake occurrence

Previous studies have reported that large earthquakes preferentially occur in association with negative TPGA in forearc areas (Song & Simons 2003; Wells *et al*. 2003). According to this concept, the implied seismic potential is higher for the Sumatra and lower for the Java subduction zone with negative and positive TPGA, respectively (Grevemeyer & Tiwari 2006). As defined by Song & Simons (2003), the TPGA is calculated as the original free-air gravity data minus an average regional trench-normal gravity profile. Thus, large-amplitude variations in the TPGA should be caused by variations in subsurface structures. Song & Simons (2003) also suggested that the frictional properties of plate interfaces represent the dominant control on variations in forearc gravity and seismogenic behaviour. This frictional interface is known as the interseismic coupling zone and is assumed to be an important factor in determining the magnitude of earthquakes (Seno 2005; Grevemeyer & Tiwari 2006; Chileh *et al*. 2008; Konca *et al*. 2008). Is there any connection between these factors? Here, according to the H_m results (Fig. 4) and subsurface structural characteristics (Fig. 6), we propose a hypothesis that relates gravity, mantle lithosphere buoyancy and the TPGA to one another and the occurrence of large earthquakes.

In strong plate coupling cases, we found that the serpentinized mantle materials cannot rise to shallow depths (Figs 6a and c), in that situation, they are less dense than their surroundings (normal mantle; Bostock *et al*. 2002; Hyndman & Peacock 2003), which can result in a relatively low gravity anomaly and negative TPGA (according to the definition of TPGA). This feature also has been observed in the Cascadia subduction zone (Bostock *et al*. 2002; Brocher *et al*. 2003; Blakely *et al*. 2005). On the other hand, in weak plate coupling cases, the density of the uplifted serpentinized mantle materials is higher than that in the ambient crust (Figs 6b and d), which can result in a relatively high gravity anomaly and positive TPGA in forearc regions. These observations illustrate that the TPGA may be related to the strength of plate coupling. The physical factors governing these characteristics would thus be most prominent in explaining why great subduction zone earthquakes are spatially correlated with the locations of gravity lows. In addition, this hypothesis is consistent with the statistical observation of Song & Simons (2003) and ties together several mechanisms by linking the driving factors of plate coupling, such as the serpentinization of mantle materials and forearc geometry. Overall, strong plate coupling, strongly negative TPGA and the potential occurrence of large earthquakes are all positively correlated. The features we observe (i.e. strong and/or weak coupling) that control seismogenic behaviour may explain similar features observed elsewhere (Fig. 4).

6 CONCLUSIONS

Assessing the potential for large earthquakes in subduction zones has always been a very important scientific and societal issue. In this study, integrating the mantle lithosphere buoyancy estimation results (published and new), subsurface structural evidence and earthquake distribution characteristics, we find that patterns of variation in H_m are closely related to earthquake magnitude. The strength of plate coupling inferred from H_m estimation can well explain the different seismogenic behaviours observed in the Sumatra and Java subduction zones. In addition, the strength of plate coupling controls the present position of serpentinized forearc mantle peridotite. The location of serpentinized mantle may be the major factor that influences the variations of the TPGA in forearc regions. This observation provides an alternative means of explaining the relationship between the occurrence of large earthquakes and negative TPGA. Integrating all observation and estimation results, we propose that strong plate coupling, strongly negative TPGA and the potential occurrence of large earthquakes in subduction zones are all positively correlated. Determining H_m, therefore, could be a consistent method of assessing large earthquake potential in subduction zones.

ACKNOWLEDGEMENTS

Constructive reviews from two anonymous reviewers are appreciated. We also thank D. Brown for his helpful discussions and comments. This research was mainly supported by the Ministry of Science and Technology of Taiwan (MOST 108-2116-M-008-007). Figures in this paper were generated using the Generic Mapping Tool (GMT).

REFERENCES

Abercrombie, R.E., Antolik, M., Felzer, K. & Ekström, G., 2001. The 1994 Java tsunami earthquake: slip over a subducting seamount, *J. geophys. Res.,* **106,** 6595–6607.

Ando, M., Nakamura, M., Matsumoto, T., Furukawa, M., Tadokoro, K. & Furumoto, M., 2009. Is the Ryukyu subduction zone in Japan coupled or decoupled?—The necessity of seafloor crustal deformation observation, *Earth Planets Space,* **61,** 1031–1039.

Blakely, R.J., Brocher, T.M. & Wells, R.E., 2005. Subduction-zone magnetic anomalies and implications for hydrated forearc mantle, *Geology,* **33,** 445–448.

Bostock, M.G., Hyndman, R.D., Rondenay, S. & Peacock, S.M., 2002. An inverted continental Moho and serpentinization of the forearc mantle, *Nature,* **147,** 536–538.

Brizzi, S., Sandri, L., Funiciello, F., Corbi, F., Piromallo, C. & Heuret, C., 2018. Multivariate statistical analysis to investigate subduction zone parameters favoring the occurrence of great earthquakes, *Tectonophysics,* **728,** 92–103.

Brocher, T.M., Parsons, T., Tréhu, A.M., Snelson, C.M. & Fisher, M.A., 2003. Seismic evidence for widespread serpentinized forearc upper mantle along Cascadia margin, *Geology,* **31,** 267–270.

Chlieh, M., Avouac, J.P., Sieh, K., Natawidjaja, D.H. & Galetzka, J., 2008. Heterogeneous coupling of the Sumatra megathrust constrained by geodetic and paleogeodetic measurements, *J. geophys. Res.,* **113,** B05305, doi:10.1029/2007JB004981.

DeMets, C., Gordon, R.G., Argus, D.F. & Stein, S., 1994. Effect of recent revisions to the geomagnetic reversal time scale on estimates of current plate motions, *Geophys. Res. Lett.,* **21,** 2191–2194.

Doo, W.-B., Lo, C.-L., Kuo-Chen, H., Brown, D. & Hsu, S.-K., 2015. Exhumation of serpentinized peridotite in the northern Manila subduction zone inferred from forward gravity modeling, *Geophys. Res. Lett.,* **42,** doi:10.1002/2015GL065705.

Doo, W.-B., Lo, C.-L., Wu, W.-N., Lin, J.-Y., Hsu, S.-K., Huang, Y.-S. & Wang, H.-F., 2018. Strength of plate coupling in the southern Ryukyu subduction zone, *Tectonophysics,* **723,** 223–228.

Dziewonski, A. M., Chou, T.-A. & Woodhouse, J. H., 1981. Determination of earthquake source parameters from waveform data for studies of global and regional seismicity, *J. geophys. Res.,* **86,** 2825–2852.

Grevemeyer, I. & Tiwari, V.M., 2006. Overriding plate controls spatial distribution of megathrust earthquakes in the Sunda–Andaman subduction zone, *Earth planet. Sci. Lett.,* **251,** 199–208.

Gvirtzman, Z. & Nur, A., 1999a. Plate detachment, asthenosphere upwelling, and topography across subduction zones, *Geology,* **27,** 563–566.

Gvirtzman, Z. & Nur, A., 1999b. The formation of Mount Etna as the consequence of slab rollback, *Nature,* **401,** 782–785.

Gvirtzman, Z. & Nur, A., 2001. Residual topography, lithospheric structure and sunken slabs in the central Mediterranean, *Earth planet. Sci. Lett.,* **187,** 117–130.

Heuret, A., Conrad, C.P., Funiciello, F., Lallemand, S. & Sandri, L., 2012. Relation between subduction megathrust earthquakes, trench sediment thickness and upper plate strain, *Geophys. Res. Lett.,* **39,** L05304, doi:10.1029/2011GL050712.

Hsu, S.-K., 2001. Lithospheric structure, buoyancy and coupling across the southernmost Ryukyu subduction zone: an example of decreasing plate coupling, *Earth planet. Sci. Lett.,* **186,** 471–478.

Hsu, Y.-J., Yu, S.-B., Song, T.-R.A. & Bacolcol, T., 2012. Plate coupling along the Manila subduction zone between Taiwan and northern Luzon, *J. Asian Earth Sci.,* **51,** 98–108.

Hyndman, R.D. & Peacock, S.M., 2003. Serpentinization of the forearc mantle, *Earth planet. Sci. Lett.,* **212,** 417–432.

Hyndman, R.D., Yamano, M. & Oleskevich, D.A., 1997. The seismogenic zone of subduction thrust faults, *Island Arc,* **6,** 244–260.

Kanamori, H., 1986. Rupture process of subduction zone earthquakes, *Annu. Rev. Earth Planet. Sci.,* **14,** 293–322.

Konca, A.O. *et al.*, 2008. Partial rupture of a locked patch of the Sumatra megathrust during the 2007 earthquake sequence, *Nature,* **456,** 631–635.

Kopp, H., 2013. Invited review paper: the control of subduction zone structural complexity and geometry on margin segmentation and seismicity, *Tectonophysics,* **589,** 1–16.

Lachenbruch, A.H. & Morgan, P., 1990. Continental extension, magmatism and elevation; formal relations and rules of thumb, *Tectonophysics,* **174,** 39–62.

Lo, C.-L., Doo, W.-B., Kuo-Chen, H. & Hsu, S.-K., 2017. Plate coupling across the northern Manila subduction zone deduced from mantle lithosphere buoyancy, *Phys. Earth planet. Inter.,* **273,** 50–54.

Müller, R.D., Sdrolias, M., Gaina, C. & Roest, W.R., 2008. Age, spreading rates and spreading symmetry of the world's ocean crust, *Geochem. Geophys. Geosyst.,* **9,** Q04006, doi:10.1029/2007GC001743.

Nakamura, M., 2009. Fault model of the 1771 Yaeyama earthquake along the Ryukyu Trench estimated from the devastating tsunami, *Geophys. Res. Lett.,* **36,** L19307, doi:10.1029/2009GL039730.

Natawidjaja, D.H. *et al.*, 2004. Paleogeodetic records of seismic and aseismic subduction from central Sumatran microatolls; Indonesia, *J. geophys. Res.,* **109,** B04306, doi:10.1029/2003JB002398.

Natawidjaja, D.H. *et al.* 2006. Source parameters of the great megathrust earthquakes of 1797 and 1833 inferred from coral microatolls, *J. geophys. Res.,* **111,** B06403, doi:10.1029/2005JB004025.

Newcomb, K. & McCann, W., 1987. Seismic history and seismotectonics of the Sunda Arc, *J. geophys. Res.,* **92,** 421–439.

Nishikawa, T. & Ide, S., 2014. Earthquake size distribution in subduction zones linked to slab buoyancy, *Nat. Geosci.,* **7,** 904–908.

Peacock, S.M. & Hyndman, R.D., 1999. Hydrous minerals in the mantle wedge and the maximum depth of subduction thrust earthquakes, *Geophys. Res. Lett.,* **26,** 2517–2520.

Pilchin, A., 2005. The role of serpentinization in exhumation of high- to ultra-high-pressure metamorphic rocks, *Earth planet. Sci. Lett.,* **237,** 815–828.

Ruff, L. & Kanamori, H., 1980. Seismicity and the subduction process, *Phys. Earth planet. Inter.,* **23,** 240–252.

Ruff, L.J., 1989. Do trench sediments affect great earthquake occurrence in subduction zone? *Pure appl. Geophys.,* **129,** 263–282.

Satake, K., 2015. Geological and historical evidence of irregular recurrent earthquakes in Japan, *Phil. Trans. R. Soc. A,* **373,** 20140375, doi:10.1098/rsta.2014.0375.

Scholl, D.W., Kirby, S.H. & von Hucnc, R., 2011. Exploring a link between great and giant megathrust earthquakes and relative thickness of sediment and eroded debris in the subduction channel to roughness of subducted relief, in *AGU Fall Meeting Abstract TI4B-01*, AGU, San Francisco, CA.

Scholl, D.W., Kirby, S.H., von Hucnc, R., Ryan, H., Wells, R.E. & Geist, E.L., 2015. Great ($\geq M_W 8.0$) megathrust earthquakes and the subduction of excess sediment and bathymetrically smooth seafloor, *Geosphere,* **11**(2), 236–265.

Seno, T., 2005. Variation of the downdip limit of the seismogenic zone near the Japanese Islands: Implications for the serpentinization mechanism of the forearc mantle wedge, *Earth planet. Sci. Lett.,* **231,** 249–262.

Seno, T., 2017. Subducted sediments thickness and Mw9 earthquakes, *J. geophys. Res.,* **122,** 470–491.

Simoes, M., Avouac, J.P., Cattin, R. & Henry, P., 2004. The Sumatra subduction zone: a case for a locked fault zone extending into the mantle, *J. geophys. Res.,* **109,** B10402, doi:10.1029/2003JB002958.

Song, T.R.A. & Simons, M., 2003. Large trench-parallel gravity variations predict seismogenic behavior in subduction zones, *Science,* **301,** 630–633.

Tadokoro, K., Nakamura, M., Ando, M., Kimura, H., Watanabe, T. & Matsuhiro, K., 2018. Interplate coupling state at the Nansei-Shoto (Ryukyu) trench, Japan, deduced from seafloor crustal deformation measurements, *Geophys. Res. Lett.,* **45,** doi:10.1029/2018GL078655.

Theunissen, T., Font, Y., Lallemand, S. & Liang, W.-T., 2010. The largest instrumentally recorded earthquake in Taiwan: revised location and magnitude, and tectonic significance of the 1920 event, *Geophys. J. Int.,* **183,** 1119–1133.

Uyede, S. & Kanamori, H., 1979. Back-arc opening and the mode of subduction, *J. geophys. Res.,* **84,** 1049–1061.

Wells, R.E., Blakely, R.J., Sugiyama, Y., Scholl, D.W. & Dinterman, P.A., 2003. Basin-centered asperities in great subduction zone earthquakes: a link between slip, subsidence, and subduction erosion? *J. geophys. Res.,* **108,** 2507, doi:10.1029/2002JB002072.

Zhao, D., 2001. Seismological structure of subduction zones and its implications for arc magmatism and dynamics, *Phys. Earth planet. Inter.,* **124,** 197–214.

Zhao, D., Wang, K., Rogers, G.C. & Peacock, S.M., 2001. Tomographic image of low *P* velocity anomalies above slab in northern Cascadia subduction zone, *Earth Planets Space,* **53,** 285–293.